Symmetry protected weak topological phases in a superlattice

Takahiro FUKUI, Ken-Ichiro IMURA[1] and Yasuhiro HATSUGAI [2]

Department of Physics, Ibaraki University, Mito 310-8512, Japan
[1]*Department of Quantum Matter, AdSM, Hiroshima University, Higashi-Hiroshima 739-8530, Japan*
[2]*Institute of Physics, University of Tsukuba, 1-1-1 Tennodai, Tsukuba, Ibaraki 305-8571, Japan*

(Received)

We explore novel topological phases realized in a superlattice system based on the Wilson-Dirac model. Our main focus is on a two-dimensional analogue of the weak topological insulator phases. We find such phases as are characterized by gapless edge states that are protected by symmetry but in a way sensitive to the relative orientation of the edge to the superlattice structure. We show that manifest and hidden reflection symmetries protect such weak topological phases, and propose bulk $\mathbb{Z}_2$ indices responsible for the topological protection of the edge states.

KEYWORDS: topological insulator, superlattice, Chern number, weak topological phase, Wilson-Dirac model

Topological classification is a new trend in the field of condensed matter. Though realized recently to the wide community, its position is more than influential for determining future directions of the field. Beyond the Ginzburg-Landau paradigm, topological classification can be applicable for quantum liquids without fundamental symmetry breaking.[1,2] Still truly generic systems are boring and the symmetry again restricts the systems. Then we have various physically interesting phases protected by symmetries. The periodic table of topological phases as an extension of the classical symmetry classes is situated at the heart of the idea.[3–8] Recently, extension of the standard classification scheme by including the diversity of topological phases protected by other types of symmetry has been investigated.[9–16]

Topological phases are mostly gapped then the bulk is characterized by the absence of low energy excitations. On the other hand, with boundaries or impurities, there exist peculiar localized modes as edge states. The emergence of the edge states is not accidental and is a fundamental property of the topological phases as the bulk-edge correspondence.[7,8,17] The edge states further reflect symmetry of the topological phases and describe their variety beyond the bulk characterization.

In this letter we attempt to further extend the idea of the topological classification to a superlattice version of the Wilson-Dirac type lattice model that exhibits hidden reflection symmetry. Motivation of this work is by no means purely academic. Now that basic understanding of simple topological insulator crystals has been established, a possible direction of not only the theoretical but the experimental research is to seek for the diversity of topological quantum phenomena. Recently, multilayer heterostructures consisting of alternating layers of topological and ordinary insulators have been experimentally realized, exhibiting an interesting correlation of bulk and surface properties.[18,19]

This letter highlights a two-dimensional (2D) analogue of such a superlattice system; a variant of the Wilson-Dirac type tight-binding model with a stripe structure (see Fig. 1). Without such a spatial non-uniformity the simple 2D Wilson-Dirac model is known as a typical $\mathbb{Z}$-type model specified by the Chern number.[20] Extension of this model to the quantum spin Hall effect (QSHE)[21] has been carried out,[22] in which the $\mathbb{Z}_2$ invariant[23,24] distinguishes the QSHE phase and trivial phase.

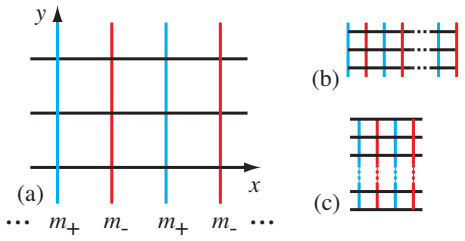

Fig. 1. The superlattice structure: (a) schematic illustration of the lattice, (b-c) different types of ribbon geometry. The two edges of the ribbon are along the *y*-axis in (b), while along the *x*-axis in (c).

Here, we demonstrate that the superlattice version exhibits a richer phase diagram (see Fig. 2) that cannot be classified by a single topological invariant. Since the mass parameter m controls the Chern number c in the *uniform* system, the superlattice of the mass (m_+, m_-) can be regarded as that of distinct Chern insulators (c_+, c_-). On the other hand, this model has the total Chern number C in its own right. We find that in the $C = 0$ sector there appear a 2D analogue of weak topological insulating phases[25–27] characterized by anisotropic topological properties. Although it is gapless as a two dimensional system, we mention here similarity of graphene where there exist direction dependent boundary states with time reversal symmetry ($C = 0$).[28,29]

Figure 1 shows schematic configuration of the superlattice model considered from now on. The model is defined on a square lattice, and on each site $\boldsymbol{r} = (x, y)$ of the lattice the electron is allowed to occupy two orbital (pseudo-spin) states with which a set of Pauli matrices σ_μ ($\mu = x, y, z$) is associated. The Hamiltonian is defined by

$$H = \sum_{\boldsymbol{r}} \left[\sum_{\mu=x,y} \left(|\boldsymbol{r}\rangle \Gamma_\mu \langle \boldsymbol{r} + \hat{\boldsymbol{\mu}}| + |\boldsymbol{r} + \hat{\boldsymbol{\mu}}\rangle \Gamma_\mu^\dagger \langle \boldsymbol{r}| \right) + |\boldsymbol{r}\rangle V(\boldsymbol{r}) \langle \boldsymbol{r}| \right], \tag{1}$$

where $\hat{\boldsymbol{\mu}}$ stands for the unit vector to the μ-direction, and the hopping and the on-site potential terms are specified as

$$\Gamma_\mu = -\frac{it}{2}\sigma_\mu + \frac{b}{2}\sigma_z,$$

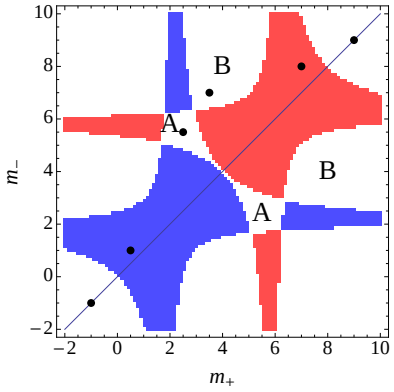

Fig. 2. Phase diagram of the superlattice model for $b = 2$ and $t = 1$: Chern number C evaluated at each point on the (m_+, m_-)-plane is indicated by different colors: blue: $C = 1$, red: $C = -1$ and white: $C = 0$. Thick black dots correspond to the reference points in Table II.

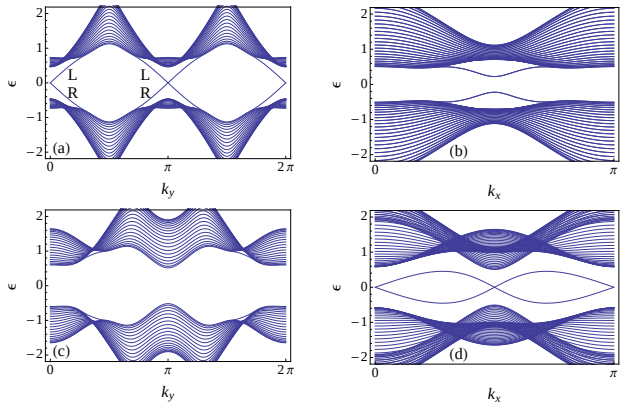

Fig. 3. Energy spectrum in the ribbon geometry: $b = 2$, $t = 1$ with boundaries along the y- (left) and x- (right) directions. The upper [lower] panels: (a), (b) [(c), (d)] correspond to the case of mass parameters $m_+ = 2.5$, $m_- = 5.5$ [$m_+ = 3.5$, $m_- = 7$] belonging to the phase A [B]. In (a), the suffix L and R indicate that the corresponding edge state is localized at the left or right boundary in Fig. 1 (b).

$$V(\boldsymbol{r}) = [m + (-1)^x \delta m - 2b]\,\sigma_z \equiv (m_\pm - 2b)\,\sigma_z. \qquad (2)$$

Notice that the lattice constant has been chosen to be unity, and hence, x and y take only integral values. In this letter we focus on the simplest superlattice structure as depicted in Fig. 1 in which $V(\boldsymbol{r})$ takes two alternating values on each column of the vertical stripe. Taking into account a doubling of the unit cell due to the stripe texture as a sub-lattice degree of freedom, one can block-diagonalize eq. (1) in the reciprocal space as $H = \sum_{\boldsymbol{k}} |\boldsymbol{k}\rangle \mathcal{H}(\boldsymbol{k}) \langle \boldsymbol{k}|$ whose matrix element $\mathcal{H}(\boldsymbol{k})$ is given by

$$\mathcal{H}(\boldsymbol{k}) = \begin{pmatrix} M_+ + t \sin k_y \sigma_y & \Gamma_x + e^{-2ik_x}\Gamma_x^\dagger \\ \Gamma_x^\dagger + e^{2ik_x}\Gamma_x & M_- + t \sin k_y \sigma_y \end{pmatrix}, \qquad (3)$$

where different rows and columns specify the sub-lattice, *i.e.*, whether the electron is on a blue column (x: even) or on a red one (x: odd) in Fig. 1 (a), and $M_\pm = \Big[m_\pm + b(\cos k_y - 2)\Big]\sigma_z$.

The uniform line, $m_+ = m_- = m$ ($\delta m = 0$), corresponds to the standard Wilson-Dirac model:[20,22] $\mathcal{H}(\boldsymbol{k}) = t \sum_\mu \sin k_\mu \sigma_\mu + m(\boldsymbol{k})\sigma_z$, where $m(\boldsymbol{k}) = [m + b \sum_\mu (\cos k_\mu - 1)]\sigma_z$. The half-filled ground state of the model is classified by the Chern number[30,31] C that takes a nontrivial value $C = 1$ when $0 < m/b < 2$, while $C = -1$ when $2 < m/b < 4$ [otherwise C takes a trivial value ($C = 0$)]; change of the topological number corresponds to closing of the gap [zeros of $m(\boldsymbol{k})$] at the Dirac point $\boldsymbol{k} = (0, 0)$ and at its doublers' points $(\pi, 0), (\pi, \pi), (0, \pi)$. Away from the uniform line it is still possible to compute the Chern number C by applying the prescription given in Ref.[32] to the present superlattice model. A phase diagram thus obtained is shown in Fig. 2.

It has the following specific features: Topologically nontrivial phases with nonzero Chern numbers $C = \pm 1$ extend from the uniform line to a region of $m_+ \neq m_-$. The regions of $C = \pm 1$ overlap; at least they look like doing so in the phase diagram, to form a finite domain of $C = 0$ phase represented by A in Fig. 2. There appear other $C = 0$ phases in different parts of the phase diagram separated by topologically nontrivial phases. Are these $C = 0$ phases simply topologically trivial? Our answer is "No", in the phases represented by "A" and "B". These phases exhibit gapless edge states in the ribbon geometry [panels (a) and (d) of Fig. 3]. Interestingly, the way these edge states appear depends on the way the system's boundaries are introduced (compare the top and bottom rows of Fig. 3). The structure of the phase diagram, especially the shape of the regions A and B is strongly dependent on the hopping amplitude t in contrast to the phase boundaries on the uniform line: $m_+ = m_-$.[33] It should be emphasized that though the concrete arrangement of distinct regions shown in Fig. 2 is not generic and varies continuously as a function of t, the behavior of the edge states in the two types of $C = 0$ phases A and B are generic, implying that they are protected by some symmetry.

The concept of the bulk-edge correspondence is now established,[17,34–36] dictating that the topological property of the bulk is fully reflected in the spectrum of the edge states. In the remainder of this letter we show that the gapless edge modes found in the $C = 0$ phases A and B are indeed topologically protected, and interpret the corresponding $C = 0$ phases as a 2D analogue of the weak topological insulator in 3D.[25–27] Figure 3 highlights the "weak" nature of the phases A and B.

In the phase A, edge states appear at the boundaries parallel to the y-axis [Fig. 3 (a)], whereas no edge states appear along those parallel to the x-axis [Fig. 3 (c)]. As indicated in Fig. 3 (a) a pair of counter-propagating modes; one localized at the left boundary (L) and the other at the right boundary (R), cross at the zero energy, and also at a specific value of the momentum (symmetric point), either at $k_y = 0$ or $k_y = \pi$. As we will show soon, this phase is reminiscent of the QSHE, since $C = c_+ + c_- = 0$ for $c_+ = 1$ and $c_- = -1$, and one pair of edge states are due to $c_+ = 1$, and the others due to $c_- = -1$. In passing, we mention that in the present model, the existence of particle-hole and inversion (or reflection) symmetries ensures the spectrum at each $\boldsymbol{k}$ to be symmetric with respect to zero. This is also the case with the edge spectrum.

The phase B is, on the other hand, understood by considering the limit $m_- \to \infty$. We will claim that the mid-gap states in Fig. 3 (d) can be deformed into topologically protected flat bands in this limit. To be concrete, when $m_- \to \infty$, electron occupation on m_- sites is suppressed, and the model reduces to just a set of isolated one-dimensional ladders described by

Table I. Non-zero coefficients of the Hamiltonian (6).

α_1	$t\sin k_x$	β_1	$b\cos k_x$
α_2	$t\sin k_y$	β_5	δm
α_3	$\left[m+b(\cos k_y-2)\right]$		

a reduced Hamiltonian,

$$\mathcal{H}(k_y) = t\sin k_y\sigma_y + \left[m_+ + b(\cos k_y - 2)\right]\sigma_z, \tag{4}$$

Owing to chiral symmetry of this Hamiltonian, the Berry phase integrated over k_y is quantized to 0 or π.[29] To see this, set $Y = t\sin k_y$ and $Z = m_+ + b(\cos k_y - 2)$. Then, if the origin $(0,0)$ is located inside the ellipse (Y,Z) forms in the Y-Z plane, i.e., $1 < m_+/b < 3$, the Berry phase is π (nontrivial) in which the zero energy flat bands are expected.[29] Thus the isolated mid-gap states in Fig. 3 (d) can be deformed without the bulk gap closing to these topologically protected flat bands. Indeed, in the phase diagram in Fig. 2 the blue and red regions become narrower as $m_- \to \infty$, converging respectively to a linear region on $m_+ = 2$ and on $m_+ = 6$.

What is a bulk topological invariant characterizing these weak topological phases embedded in $C = 0$? In contrast to the case of the so-called $\mathbb{Z}_2$ topological insulator the present system lacks time-reversal symmetry. Yet, as we demonstrate below, the proposed weak topological phases are protected by another type of a $\mathbb{Z}_2$ invariant associated with manifest as well as *hidden* reflection symmetry. To see this, it is convenient to introduce a unitary-transformed Hamiltonian:

$$\widetilde{\mathcal{H}}(\boldsymbol{k}) = U(k_x)\mathcal{H}(\boldsymbol{k})U^\dagger(k_x),$$
$$U(k_x) = \mathbb{1}_2 \otimes \mathrm{diag}(1, e^{-\mathrm{i}k_x}), \tag{5}$$

where $\mathbb{1}_2$ operates on the Pauli matrices. The transformed Hamiltonian $\widetilde{\mathcal{H}}(\boldsymbol{k})$ is represented simply as

$$\widetilde{\mathcal{H}}(\boldsymbol{k}) = \alpha_\mu\gamma_\mu + \beta_\mu\gamma_{2\mu}, \tag{6}$$

where γ-matrices are defined by $\gamma_1 = \sigma_x\otimes\sigma_x$, $\gamma_2 = \sigma_y\otimes\mathbb{1}_2$, $\gamma_3 = \sigma_z\otimes\mathbb{1}_2$, $\gamma_4 = \sigma_x\otimes\sigma_y$, $\gamma_5 = \sigma_x\otimes\sigma_z$, and $\gamma_{\mu\nu} \equiv \mathrm{i}[\gamma_\mu,\gamma_\nu]/2$. Coefficients α_μ and β_μ are listed in Table I.

We begin by demonstrating the following two properties: (i) $\widetilde{\mathcal{H}}(\boldsymbol{k})$ possesses not only particle-hole symmetry but also reflection (inversion) symmetry, and (ii) $\widetilde{\mathcal{H}}(\boldsymbol{k})$ is not periodic with respect to k_x, $\widetilde{\mathcal{H}}(k_x+\pi,k_y) = U(\pi)\widetilde{\mathcal{H}}(k_x,k_y)U^\dagger(\pi)$. Here, the form of $U(\pi) = \mathbb{1}_2\otimes\sigma_z$ implies that a twisted boundary condition is imposed on the Hamiltonian $\widetilde{\mathcal{H}}(\boldsymbol{k})$. Nevertheless, the half-filled ground states of $\widetilde{\mathcal{H}}(\boldsymbol{k})$ and $\mathcal{H}(\boldsymbol{k})$ give the same Chern number on the same Brillouin zone $[0,\pi]\otimes[0,2\pi]$.

(i) Let us first note that the Hamiltonian (6) has particle-hole symmetry,

$$\Xi\widetilde{\mathcal{H}}(\boldsymbol{k})\Xi^{-1} = -\widetilde{\mathcal{H}}(-\boldsymbol{k}), \tag{7}$$

where $\Xi = -\mathrm{i}\gamma_2\gamma_3 K = \sigma_1\otimes\mathbb{1}_2 K$ and K is the complex conjugation operator. The presence of this symmetry is rather natural if one recalls that eq. (1) is a straight-forward extension of the Wilson-Dirac Hamiltonian. The model has other symmetries prescribed as

$$P_y\widetilde{\mathcal{H}}(k_x,k_y)P_y^{-1} = \widetilde{\mathcal{H}}(-k_x,k_y), \tag{8}$$

$$P_x\widetilde{\mathcal{H}}(k_x,k_y)P_x^{-1} = \widetilde{\mathcal{H}}(k_x,-k_y), \tag{9}$$

where $P_y = \gamma_3 K$ and $P_x = K$. These may be regarded as (anti-unitary) reflection symmetry with respect to y- and x-direction, respectively, and therefore, the model has inversion symmetry $P\widetilde{\mathcal{H}}(\boldsymbol{k})P^{-1} = \widetilde{\mathcal{H}}(-\boldsymbol{k})$, where $P = P_xP_y = \gamma_3$. Symmetries (7) and (8) are manifest also in $\mathcal{H}(\boldsymbol{k})$, but the symmetry (9) is hidden in $\mathcal{H}(\boldsymbol{k})$.

(ii) We introduce the Chern number $\widetilde{C}$ in the transformed basis. Let $\widetilde{\psi}(k)$ be the negative energy multiplet of the Hamiltonian $\widetilde{\mathcal{H}}(\boldsymbol{k})$ with a phase convention,

$$\widetilde{\psi}(-k_x,k_y) = P_y\widetilde{\psi}(k_x,k_y),$$
$$\widetilde{\psi}(k_x,-k_y) = P_x\widetilde{\psi}(k_x,k_y). \tag{10}$$

Note that the periodicity of the wave functions is such that $\widetilde{\psi}(k_x+\pi,k_y) = U(\pi)\widetilde{\psi}(k_x,k_y)$, where $U(\pi) = -\mathrm{i}\gamma_1\gamma_4$. Let $\widetilde{A}_i = \widetilde{\psi}^\dagger\partial_i\widetilde{\psi}$ and $\widetilde{F}_{12} = \epsilon_{ij}\mathrm{tr}\partial_i\widetilde{A}_j$ be the Berry connection and curvature, respectively, where $\partial_i \equiv \partial_{k_i}$. Because of eqs. (10), these obey

$$\widetilde{A}_j(-k_x,k_y) = (-)^{j-1}\widetilde{A}_j(k_x,k_y),$$
$$\widetilde{A}_j(k_x,-k_y) = (-)^j\widetilde{A}_j(k_x,k_y),$$
$$\widetilde{F}_{12}(-k_x,k_y) = \widetilde{F}_{12}(k_x,-k_y) = \widetilde{F}_{12}(k_x,k_y). \tag{11}$$

The Chern number $\widetilde{C}$ of the half-filled states is given by the integration of $\widetilde{F}_{12}(k)$ over the Brillouin zone. Let us verify $\widetilde{C} = C$, where C is defined in terms of the wave function $\psi(\boldsymbol{k})$ of the original Hamiltonian $\mathcal{H}(\boldsymbol{k})$ in (3). The two wave functions can be related as $\widetilde{\psi}(\boldsymbol{k}) = U(k_x)\psi(\boldsymbol{k})$. This implies $\widetilde{A}_i = A_i + \psi^\dagger U^\dagger\partial_i U\psi$, and hence, $\widetilde{F}_{12} = F_{12} + \epsilon_{ij}\partial_i(\mathrm{tr}P_-U^\dagger\partial_j U)$, where A_i and F_{12} are the Berry connection and curvature defined through $\psi(\boldsymbol{k})$, and $P_-(\boldsymbol{k})$ is the projection operator to the occupied states, $P_-(\boldsymbol{k}) = \psi(\boldsymbol{k})\psi^\dagger(\boldsymbol{k})$. Then, since $U^\dagger\partial_1 U = -\mathrm{i}\mathbb{1}_2\otimes\mathrm{diag}(0,1)$ is a constant matrix and $P_-(\boldsymbol{k})$ is gauge-invariant as well as periodic on the Brillouin zone, the above difference term between $\widetilde{F}$ and F vanishes if it is integrated over the Brillouin zone owing to the Stokes theorem on the torus. Thus, we reach $\widetilde{C} = C$.

Based on the properties (i) and (ii), let us consider a topological invariant that characterizes the weak topological phase studied so far. Consider the Berry connection $\widetilde{A}_i$. Because of (10), the obstruction of the gauge-fixing occurs mainly along the four symmetry lines $k_x = 0,\pi/2$ and $k_y = 0,\pi$. Namely, if the Berry connection is plotted on the Brillouin zone, vortices can appear on these lines. Moreover, they are always paired because of (11). For example, on the Brillouin zone defined by $[0,\pi]\otimes[0,2\pi]$, a pair on $k_x = 0$ line sit on the points $(0,k_y^\star)$ and $(0,2\pi-k_y^\star)$ with the same vorticity. Of course, in some other points away from these symmetry lines, there can also occur obstructions. In this case, vortices appear "in quartets" which are symmetric with respect to four symmetry lines. These have also the same vorticity. Thus we know that even number of vortices always appear as long as the phase convention (10) is adopted. However, there are exceptions: The four crossing points of the four symmetry lines, i.e., $(0,0)$, $(\pi/2,0)$, $(\pi/2,\pi)$, and $(0,\pi)$, which will be referred to as $X_1,\cdots,X_4$ in this order. On these points, single vortices can appear. These single vortices cannot move away from these points even if one makes local gauge transformation, since if they did so, they would need an odd number of partners, as

Table II. The $\mathbb{Z}_2$ invariant numerically computed. The top two cases correspond to the uniform mass Wilson-Dirac model $\delta m = 0$ ($b = 2$ and $t = 1$) in the trivial $C = 0$ phase, whereas the middle two cases are for $C = \pm 1$ phases. The bottom two cases are for the weak topological phase A and B. These six cases are indicated as black points in Fig. 2.

m_+	m_-	C	$[n_1n_2n_3n_4]$	$[[\tilde{n}_1\tilde{n}_2\tilde{n}_3\tilde{n}_4]]$
−1	−1	0	[0110]	[[0000]]
9	9	0	[0110]	[[0000]]
0.5	1	1	[1110]	[[1000]]
7	8	−1	[0111]	[[0001]]
2.5	5.5	0	[1111]	[[1001]]
3.5	7	0	[0101]	[[0011]]

discussed above. Indeed, in the phase $C = \pm 1$ in Fig. 2, odd number of vortices are located on these four symmetry points $\{X_i\}$ in any gauge, as long as the phase convention (10) is used. See Table II.

This implies that unpaired vortices on these points can be used to reveal the topological properties of the present system. Indeed, it informs us of the "parity" of the Chern number. Moreover, different configurations of vortices on $\{X_i\}$ imply topologically different phases, since the location of these vortices are gauge invariant. Therefore, it is natural to expect that the $C = 0$ phase can be further distinguished by the obstruction on the four symmetry points. Notice that the present Hamiltonian $\widetilde{\mathcal{H}}$ has inversion symmetry. Therefore, the obstruction on the four points $\{X_i\}$ is associated with the parity of the wavefunctions. With respect to the parity operator P, eq. (10) implies that we choose

$$\widetilde{\psi}(-k) = P\widetilde{\psi}(k). \tag{12}$$

At the point $X_1 = (0, 0)$, for example, this means that $\widetilde{\psi}(0) = P\widetilde{\psi}(0)$. Let us assume that among the two occupied wavefunctions of $\widetilde{\psi}(0)$, n wavefunctions have the parity -1 and others have $+1$. Then, the former are the obstructions of the gauge-fixing condition (12). When n is even ($n = 0$ or 2), there appear even number of the vortices on X_1, which can move away from this point via suitable gauge transformation. However, if n is odd ($n = 1$), one vortex is forced to locate on X_1. The $\mathbb{Z}_2$ invariant in this meaning can be extracted from $\det[\widetilde{\psi}^\dagger(0)P\widetilde{\psi}(0)] = \pm 1$, where the case -1 is the $\mathbb{Z}_2$ obstruction of the condition (12).

This simple observation is extended to other symmetry points X_i. Here, it should be noted that the wavefunction $\widetilde{\psi}(k)$ is not periodic with respect to k_x because of the twist operator $U(k_x)$, as discussed below (10). In particular, $\widetilde{\psi}(-k_x + \pi, \bar{k}_y) = U(\pi)\widetilde{\psi}(-k_x, \bar{k}_y) = U(\pi)P\widetilde{\psi}(k_x, \bar{k}_y)$, where $\bar{k}_y = 0$ or π, and the phase convention at $k_x = \pi/2$ is thus modified. Note that $P = \sigma_3 \otimes \mathbb{1}_2$ and $U(\pi) = \mathbb{1}_2 \otimes \sigma_3$ and hence $U(\pi)P = \sigma_3 \otimes \sigma_3$. Thus, the condition (12), taking this periodicity into account, is explicitly written as

$$\widetilde{\psi}(X_i) = P_i\widetilde{\psi}(X_i), \quad i = 1, \cdots, 4, \tag{13}$$

where $P_i \equiv \sigma_3 \otimes \mathbb{1}_2$ ($i = 1, 4$) and $P_i \equiv \sigma_3 \otimes \sigma_3$ ($i = 2, 3$). This leads to the $\mathbb{Z}_2$ obstruction

$$\delta_i = \det \widetilde{\psi}^\dagger(X_i)P_i\widetilde{\psi}(X_i), \tag{14}$$

which can take ± 1 only. Now let us define a set of four numbers $[n_1n_2n_3n_4]$, where $\delta_i = (-1)^{n_i}$. These numbers are gauge invariant modulo 2, indicating that $n_i = 1$ (0) imply obstruction (no obstruction) on X_i.

In Table II we show several examples of this invariant. Notice that even in trivial $C = 0$ phases on the $m_+ = m_-$ line, the obtained invariant is [0110], which seems nontrivial at first sight. It is, however, due to the effect of the twist operator $U(\pi)$. Roughly speaking, $U(\pi) = \mathbb{1}_2 \otimes \sigma_3$ implies that among four states, half are periodic and the other half are anti-periodic in k_x, and therefore, the half-filled ground states includes one periodic and one anti-periodic states. Therefore, we should define the relative $\mathbb{Z}_2$ invariant as "excitations" for this background obstruction such that $[[\tilde{n}_1\tilde{n}_2\tilde{n}_3\tilde{n}_4]] = [n_1n_2n_3n_4] - [0110] \bmod 2$.

This is the bulk $\mathbb{Z}_2$ invariant that characterizes the weak topological phases in the present superlattice system. From Table II, we can interpret the phase A as [[1001]] = [[1000]] + [[0001]] and thus the $C = 1 + (-1) = 0$ nature of this states is established. It is also obvious that the phase B, assigned [[0011]], is distinguished from this phase.

Let us finally mention how the $\mathbb{Z}_2$ indices $\tilde{n}_i$ are related to the edge spectrum in the two different ribbon geometries as shown in Fig. 3. Define $\tilde{\delta}_i = (-1)^{\tilde{n}_i}$. This is the relative δ_i in (14) with respect to the background. Then, in the spirit of Ref.[37] we consider a product of two $\tilde{\delta}_i$'s [$\tilde{\delta}_{\bar{k}_\mu 1}$ and $\tilde{\delta}_{\bar{k}_\mu 2}$] on a line $k_\mu = \bar{k}_\mu$ ($\bar{k}_y = 0, \pi$, while $\bar{k}_x = 0, \pi/2$), and define the quantity $\pi_{\bar{k}_\mu} = \tilde{\delta}_{\bar{k}_\mu 1}\tilde{\delta}_{\bar{k}_\mu 2}$. Again, $\pi_{\bar{k}_\mu} = \pm 1$. If $\pi_{\bar{k}_\mu} = -1$, the edge spectrum in the ribbon geometry directed to the μ-axis becomes gapless at $k_\mu = \bar{k}_\mu$, otherwise the spectrum is gapped. Here, this statement can be verified empirically using the explicit values of $\tilde{n}_i$ listed in Table II, while the proof of the statement involves calculation of the Berry curvature integrated along the loop $k_\mu = \bar{k}_\mu$ (Wilson loop). We leave detailed description of this proof to a forthcoming publication.

Acknowledgment

The authors are supported by KAKENHI; T.F. and K.I. by the "Topological Quantum Phenomena" (Nos. 23103502 and 23103511), and Y.H. by Nos. 23340112, 23654128, 23540460 and 25610101.

1) X. G. Wen: Phys. Rev. B **40** (1989) 7387.
2) Y. Hatsugai: J. Phys. Soc. Jpn. **75** (2006) 123601.
3) M. Zirnbauer: J. Math. Phys. **37** (1996) 4986.
4) A. Altland and M. Zirnbauer: Phys. Rev. **B55** (1997) 1142.
5) A. Schnyder, S. Ryu, A. Furusaki, and A. W. W. Ludwig: Phys. Rev. B **78** (2008) 195125; AIP Conf. Proc. **1134** (2009) 10.
6) A. Kitaev: AIP Conf. Proc. **1134** (2009) 22.
7) M. Z. Hasan, C. L. Kane: Rev. Mod. Phys. **82** (2010) 3045.
8) X.-L. Qi, S.-C. Zhang: Rev. Mod. Phys. **83** (2011) 1057.
9) M. Sato: Phys. Rev. B **81** (2010) 220504.
10) X. Chen, Z.-C. Gu and X. G. Wen: Phys. Rev. B **83** (2011) 035107.
11) L. Fidkowski and A. Kitaev: Phys. Rev. B **83** (2011) 075103.
12) F. Pollmann, E. Berg, A. M. Tuner and M. Oshikawa: Phys. Rev. B **85** (2012) 075125.
13) L. Fu: Phys. Rev. Lett. **106** (2011) 106802.
14) R.-J. Slager, A. Mesaros, V. Juricic and J. Zaanen: Nature Physics **9** (2013) 98.
15) Y. Ueno, A. Yamakage, Y. Tanaka and M. Sato: arXiv:1303.0202.
16) C.-K. Chiu, H. Yao, and S. Ryu: arXiv:1303.1843.
17) Y. Hatsugai: Phys. Rev. Lett. **71** (1993) 3697.
18) K. Nakayama, K. Eto, Y. Tanaka, T. Sato, S. Souma, T. Takahashi, K. Segawa, and Y. Ando: arXiv:1206.7043.
19) T. Valla, Huiwen Ji, L. M. Schoop, A. P. Weber, Z.-H. Pan, J. T. Sad-

owski, E. Vescovo, A. V. Fedorov, A. N. Caruso, Q. D. Gibson, L. Müchler, C. Felser, and R. J. Cava: arXiv:1208.2741.
20) X.-L. Qi, T. Hughes, S.-C. Zhang: Phy. Rev. B **78** (2008) 195424.
21) C. L. Kane and E. J. Mele: Phys. Rev. Lett. **95** (2005) 226801.
22) B. A. Bernevig, T. L. Hughes, and S.-C. Zhang: Science **314** (2006) 1757.
23) C. L. Kane and E. J. Mele: Phys. Rev. Lett. **95** (2005) 146802.
24) L. Fu and C. L. Kane: Phys. Rev. B **74** (2006) 195312.
25) L. Fu, C. L. Kane, and E. J. Mele: Phys. Rev. Lett. **98** (2007) 106803.
26) J. E. Moore and L. Balents: Phys. Rev. B **75** (2007) 121306.
27) R. Roy: Phys. Rev. B **79** (2009) 195322.
28) M. Fujita, K. Wakabayashi, and K. Kusakabe J. Phys. Soc. Jpn. **65** (1996) 1920.
29) S. Ryu and Y. Hatsugai: Phys. Rev. Lett. 89 (2002) 077002.
30) D. J. Thouless, M. Kohmoto, M. P. Nightingale, and M. den Nijs: Phys. Rev. Lett. **49** (1982) 405.
31) M. Kohmoto: Ann. Phys. **160** (1985) 355.
32) T. Fukui, Y. Hatsugai, and H. Suzuki: J. Phys. Soc. Jpn. **74** (2005) 1674.
33) In the presence of a superlattice structure it is observed that the structure of the phase diagram is determined by a competition of two length scales: the interval of the stripe structure and the penetration depth of the edge wave function, especially in the x-direction; the latter being a function of t. See, *e.g.*, K.-I. Imura, A. Yamakage, S. Mao, A. Hotta and Y. Kuramoto: Phys. Rev. B **82** (2010) 085118, and references therein.
34) G. E. Volovik, *The Universe in a Helium Droplet* (Oxford University Press, Oxford, 2003, §22).
35) A. M. Essin and V. Gurarie: Phys. Rev. B **84** (2011) 125132.
36) T. Fukui, K. Shiozaki, T. Fujiwara, and S. Fujimoto: J. Phys. Soc. Jpn. **81** (2012) 114602.
37) L. Fu and C. L. Kane: Phys. Rev. B **76** (2007) 045302.